Clinical Neurophysiology 130 (2019) 429–438

Contents lists available at ScienceDirect

Clinical Neurophysiology

journal homepage: www.elsevier.com/locate/clinph

Widespread interictal epileptic discharge more likely than focal discharges to unveil the seizure onset zone in EEG-fMRI

Tomohiro Yamazoe [a,b,*], Nicolás von Ellenrieder [a], Hui Ming Khoo [a,c], Yao-Hsien Huang [a,d], Natalja Zazubovits [a], François Dubeau [a], Jean Gotman [a]

[a] Montreal Neurological Institute and Hospital, McGill University, Canada
[b] Seirei Hamamatsu General Hospital, Hamamatsu, Japan
[c] Department of Neurosurgery, Osaka University Graduate School of Medicine, Suita, Japan
[d] Department of Neurology, Shuang Ho Hospital, Taipei Medical University, New Taipei, Taiwan

ARTICLE INFO

Article history:
Accepted 25 December 2018
Available online 30 January 2019

Keywords:
EEG-fMRI
Refractory focal epilepsy
Interictal epileptic discharge
Seizure onset zone
Spatial extent
Number of events

HIGHLIGHTS

- EEG-fMRI is useful to detect epileptic focus for refractory epilepsy, but is not always successful.
- Number of interictal epileptic discharges is important factor to obtain significant BOLD cluster.
- Widespread interictal discharges are more likely to localize the seizure onset zone than focal ones.

ABSTRACT

Objective: We hypothesized that the number of interictal epileptic discharges (IEDs) during scan and their spatial extent are contributing factors in obtaining appropriate activations that reveal the seizure onset zone (SOZ) in EEG-fMRI.
Methods: 157 IED types, each corresponding to one EEG scalp distribution, in 64 consecutive EEG-fMRI studies from 64 patients with refractory localization-related epilepsy were reviewed. To determine reliable activation, we used the threshold corresponding to corrected whole-brain topological false discovery rate (FDR). The location with maximum activation was compared to the presumed SOZ as defined by a comprehensive evaluation for each patient.
Results: The number of IEDs was significantly higher in the types with *t*-value above FDR than with *t*-value below FDR. The presumed SOZ could be delineated in 30 of the 64 patients. Among these patients, the types of IED concordant with the SOZ had significantly larger extent on scalp EEG than the IED types discordant with the SOZ.
Conclusions: The number of IEDs is important factor in obtaining reliable activations in EEG-fMRI. IEDs with larger spatial extent are more likely to reveal, on maximum BOLD, accurate location of the SOZ.
Significance: Widespread discharges are more likely to yield a reliable activation for SOZ in EEG-fMRI.
© 2019 International Federation of Clinical Neurophysiology. Published by Elsevier B.V. All rights reserved.

1. Introduction

Non-invasive presurgical evaluations play a crucial role to achieve good surgical outcome for patients with drug resistant epilepsy who are candidates for epilepsy surgery (Duncan et al., 2016, Shih et al., 2018). The information from non-invasive diagnostic tools can often offer successful surgical strategies, but in some cases, additional information from intracranial electroencephalography (EEG) is required to assess the epileptic generator. Intracranial EEG continues to be used in increasingly complex cases that are considered as surgical candidates, despite the progress of the non-invasive diagnostic techniques that should help to reduce the necessity of invasive studies. Without a solid hypothesis for the epileptic generator, the implantation of intracranial EEG is discouraged because of the limitations, risks and costs

Abbreviations: IEDs, interictal epileptic discharges; FDR, false discovery rate; SOZ, seizure onset zone; pSOZ, presumed seizure onset zone.

* Corresponding author at: Montreal Neurological Institute and Hospital, McGill University, 3801 University Street, Montreal, Quebec H3A2B4, Canada. Fax: +1 514 398 1952.
E-mail address: tomohiro.yamazoe@mail.mcgill.ca (T. Yamazoe).

https://doi.org/10.1016/j.clinph.2018.12.014
1388-2457/© 2019 International Federation of Clinical Neurophysiology. Published by Elsevier B.V. All rights reserved.

(Jayakar et al., 2016). A European group study showed how improved diagnostic methods resulted in improved surgical outcome with increase of seizure freedom in the past 15 years (Baud et al., 2018). However, the progress was limited and more progress is needed to provide good seizure control by resection surgery. Thus, it is necessary to obtain stronger information from noninvasive evaluation in order to build a reasonable hypothesis for the epileptic networks in each patient.

Simultaneous EEG and functional magnetic resonance imaging (fMRI), EEG-fMRI, is a noninvasive tool to detect hemodynamic changes, as the blood oxygen level dependent (BOLD) effect, in the whole brain in relation to interictal epileptic discharges (IEDs). EEG-fMRI plays a role for the localization of ictal and interictal networks that can be useful during presurgical assessment, helping with the design of intracranial EEG sampling strategies (Duncan et al., 2016). EEG-fMRI, and also magnetoencephalography (MEG), are helpful in guiding electrode implantation and surgical treatment for patients with focal cortical dysplasia, a condition that remains very difficult to treat despite the availability of new diagnostic tools (Guerrini et al., 2015). Previous studies showed that EEG-fMRI has the capacity to reveal the seizure onset zone (SOZ) in patients with drug resistant and difficult-to-localize focal epilepsy (Thornton et al., 2011, Pittau et al., 2012, Khoo et al., 2017). Removing the region of maximal BOLD activation in patients with focal epilepsy increased their likelihood of seizure freedom (An et al., 2013). However, as in most methods, results are not always significant and are not always in agreement with other localization approaches. EEG-fMRI has been shown to provide an accurate localization of the SOZ in 64–77% of patients (Pittau et al., 2012, Khoo et al., 2017). Khoo et al. (2017) report on some BOLD signal characteristics, the absolute *t*-value of the peak of the most significant BOLD cluster and the *t*-value difference between the peak of the most significant BOLD cluster and the second significant cluster, making the results accurate in over 90% of cases. However, there is no report describing the EEG factors that can affect the results of EEG-fMRI studies.

We report two characteristics of IEDs that influence the reliability of the results of EEG-fMRI studies. We hypothesized that the number of IEDs during the scan and the spatial extent of IEDs are contributing factors in obtaining activations that reveal the seizure onset zone.

2. Methods

2.1. Study population

A hundred and nine consecutive EEG-fMRI studies in patients 16 years or older acquired from April 2015 to March 2018 in our institute were reviewed retrospectively. Each patient gave written informed consent for the EEG-fMRI study, which was approved by the Research Ethic Committee of the Montreal Neurological Institute and Hospital.

2.2. EEG-fMRI acquisition, processing and analysis

EEG-fMRI acquisition, processing, and analysis were identical to that performed in previous studies (An et al., 2013, Khoo et al., 2017). EEG was recorded inside a 3 Tesla MRI scanner (Siemens Trio) with 25 MR compatible electrodes placed on the scalp using 10-20 (reference FCz) and 10-10 (F9, T9, P9, F10, T10 and P10) electrode systems. Functional images were collected in 6-min runs for a total scan of 60–90 min with patient at rest, using the following T2* - weighted echo planar imaging (EPI) sequences: repetition time (TR), 1.9 s; echo time (TE), 25 msec; 64 × 64 matrix; 33 slices; voxel, 3.7 × 3.7 × 3.7 mm; flip angle 90 degrees. IEDs with the same spatial distribution (similar or different morphologies) were grouped, whereas IEDs with different spatial distributions were considered different IED types and analyzed separately. Each IED type was characterized by its extent, defined by the number of electrodes involved in the event, assessed visually in a montage with average reference with sensitivity of 100 μV/5mm. Marking the IEDs for the analysis was performed by one reader and confirmed by a second reader. An example of IEDs with different extents is discussed in the Results (Fig. 1). Data were analyzed as an event-related design using fMRIstat (Worsley et al., 2002). Timing and duration of each IED was convolved with four hemodynamic response functions (HRFs) peaking at 3, 5, 7, and 9 s (Bagshaw et al., 2004), resulting in four regressors. Motion parameters were modeled as confounds. A combined *t*-map was created by taking, at each voxel, the most significant *t*-value from the four *t*-maps created with the four HRFs. This single combined *t* -map was used for analysis. We defined two levels of statistical significance. The first level of significance, uncorrected, was defined as a response with five contiguous voxels with $t\text{-value} \geq 3.1$ corresponding to uncorrected $p < 0.001$ for the analysis of each HRF, equivalent to uncorrected $p < 0.005$ for the combined analysis using the four HRFs (we call this "uncorrected" because it was not corrected for multiple clusters although it was corrected for the 4 HRFs) (Bagshaw et al., 2004). The second level of significance (corrected for multiple cluster comparisons) was defined by *t*-values higher than the threshold corresponding to corrected whole-brain topological false discovery rate (FDR) of 0.05 (Benjamini and Hochberg, 1995). The cluster defining threshold in the FDR computation was selected as $t \geq 3.1$. We refer to clusters that reach corrected significance level as above FDR, and to cluster that reach uncorrected but not the corrected significance level as below FDR.

For each IED type, the cluster with highest absolute *t*-value at a peak located in the cerebral cortex was defined as the primary cluster. This maximum *t*-value was compared to the thresholds defined in the previous paragraph to determine its significance level. In some analyses for EEG-fMRI, focal slow waves were assessed because these assessments could reveal SOZ, especially in pediatric patients (Jacobs et al., 2007). However, for this study, analyzed IED types with only slow waves were not considered to simplify the analysis and because they were reported to be present in only 8% of patients (Pittau et al., 2013). In the *t*-maps, a yellow-red scale corresponds to positive BOLD responses (activation) and a blue-green scale corresponds to negative responses (deactivation).

2.3. Definition of the presumed seizure onset zone

If a patient had an SEEG investigation, the presumed seizure onset zone (pSOZ) was determined by the findings from SEEG. Otherwise the pSOZ was defined by semiology, ictal EEG, interictal EEG, MR images, F-18 fluorodeoxyglucose positron emission tomography (FDG-PET), ictal single photon emission computed tomography (SPECT), and/or MEG using EEG-MEG fusion source analysis based on the Maximum Entropy of the Mean (Chowdhury et al., 2018). At first, we defined the pSOZ at the lobar level from the findings of semiology, interictal-EEG, ictal-EEG and MRI. In the patients with information about FDG-PET, ictal-SPECT and MEG, if these results were concordant with the above-mentioned pSOZ, we use them to define the pSOZ at the sublobar level. If we could not define the pSOZ from available data, we decided that the pSOZ was unknown. As a result, we could delineate pSOZ in 30 patients. After the assessment of pSOZ, the primary cluster in EEG-fMRI was compared to the pSOZ to assess their concordance at the sublobar level.

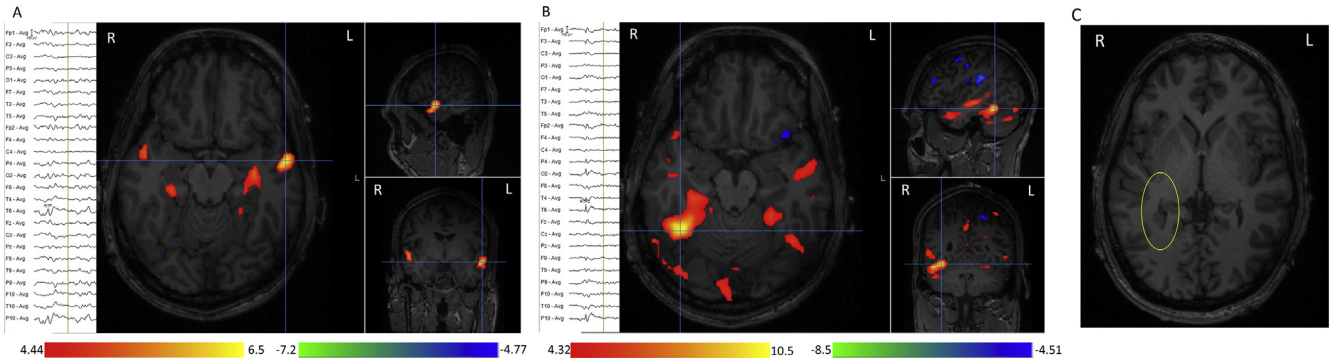

Fig. 1. Example of two primary clusters concordant and discordant with the presumed SOZ (pSOZ) in a patient (No. 22) with IEDs of different spatial extents. In the t-maps, a yellow-red scale corresponds to positive BOLD responses (activation) and a blue-green scale corresponds to negative responses (deactivation). Activation and deactivation are displayed only if above the FDR. R = right, L = left. (A) Activation from the analysis of IEDs with spatial extent in T6-P10-P4-O2. The primary cluster is in the left anterior temporal lobe, which is discordant with pSOZ. (B) Activation from the analysis of IEDs extending over T6-P10-P4-O2-T4-T10. The primary cluster is in the right fusiform gyrus, cortex close to the periventricular noduar heterotopia concordant with the pSOZ. Yellow circle showed subependimal heterotopic nodule at the inferior horn of the right lateral ventricle (C). (For interpretation of the references to colour in this figure legend, the reader is referred to the web version of this article.)

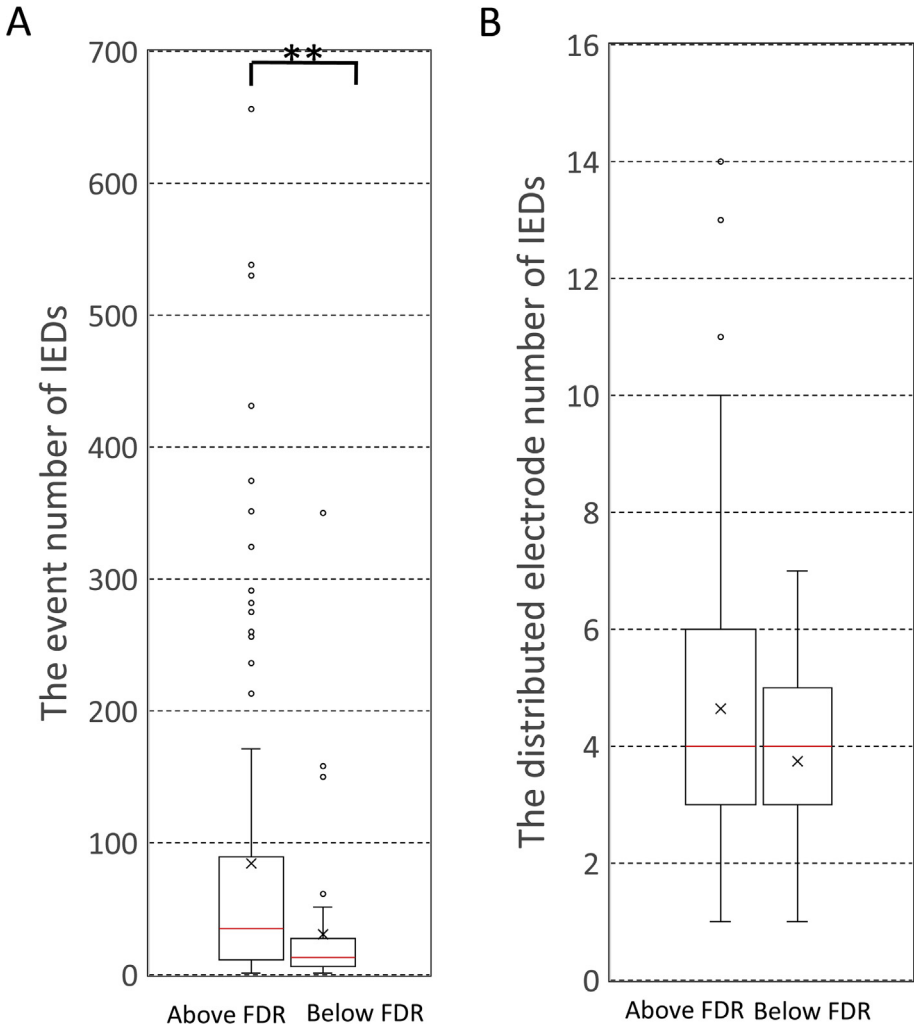

Fig. 2. The number of events and spatial extent of 157 types of IEDs in 64 studies/64 patients during EEG-fMRI and significant activations in primary clusters. The red line corresponds to the median and black boxes extend to the interquartile value. The × marks indicate the mean in each group and the black circles indicate the outliers. (A) Number of IEDs for primary clusters with *t*-value above and below FDR. The types of IEDs with *t*-value above FDR had significantly higher number of IEDs than one with t-value below FDR (**: $p < 0.0001$). (B) Spatial extent of IEDs for primary cluster with *t*-value above and below FDR. There was no significant difference in spatial extent between the two. (For interpretation of the references to colour in this figure legend, the reader is referred to the web version of this article.)

Table 1
Summary of clinical features, invesitigations, seizure localization, IEDs features, EEG-fMRI results showing the location and maximum *t*-value and its concordance with the pSOZ.

Patient ID	Spike field	Number of event	Location with maximum BOLD activation	Max *t*-value (FDR)	Concordant with pSOZ	pSOZ	MRI finding	SEEG	Seizure description (sz duration)	ictal EEG	PET	MEG
1	Fp1F3Fz	22	right temporo-occipital lobe	5.03 (4.89)	No	bifrontal interhemispheric	normal	N/A	fear aura, staring (10 s)	bifrontal	N/A	N/A
	Fp1F3FzFp2F4	97	left paracentral lobe	16.89 (4.26)	Yes							
2	T3	14	right anterior central gyrus	5.96 (4.76)	No	leftt temporal	Post surgical cavity in left anterior temporal lobe, amygdala, anterior cingulate and frontal lobe	N/A	(1) Tinnitus or strage sensation in right hemibody (a few second) (2) GTC	left temporal	N/A	N/A
	T3T5P9	13	left posterior temporal lobe	12.79 (4.74)	Yes							
3	F7T3F9T9Fp1F3C3T5P9Fz	431	left supramarginal gyrus	23.26 (4.57)	Yes	left temporal	Asymmetry of marginal area around sylvian fissure	N/A	(1) staring, right head version (2) right head version, right arm tonic movement, speech arrest (20 s)	bifrontocentral, with left dominancy	left mesial and anterior temporal	N/A
4	T3T5P9	133	leftt operculum	6.31 (4.50)	Yes	left front-temporal	Post surgical cavity in left anterior temporal lobe, amygdala-hippocumpus	N/A	(1) no aura, right head versiont, right hand dystonic posture, postictal aphasia (3 min)	left front-centro-temporal	N/A	N/A
	F3C3P3T3T5Fp1P9	20	left operculum	10 (4.39)	Yes							
	T3T5P9F3C3	324	leftt middle temporal	10.45 (4.97)	Yes							
5	F3FzFp1C3F7T3	9	left anterior insula	6.18 (4.88)	No	left temporal	atrophic left temporal lobe	N/A	(1) no aura, dysphasia (20 s) (2) staring, right arm distonic posture, quickly generalized	left front-centro-temporal	N/A	N/A
	T3T5F3C3P3F7F8T4T6P9Fp1O1FzCz	11	leftt supramarginal gyrus	8.23 (4.80)	Yes							
6	F7T3F9T9	11	right postcentral gyrus	5.25 (4.56)	No	right temporal	normal	N/A	staring, oral and bimanual automatism, right head version (3 min)	right posterior temporal	N/A	N/A
	T4T6T10P10	260	right supramarginal gyrus	7.77 (5.05)	Yes							
	F4F8T4T6F10T10P10	351	right lingual gyrus	13.42 (4.24)	Yes							
7	F7T3F9T9	530	right posterior cingulate	5.59 (4.59)	No	left temporal	left hippocumpal sclerosis	N/A	uprising heat feeling aura, dysphasia, griming with vocalization, bimanual automatism, postictal aphasia (2 min)	left front-temporal	N/A	N/A
8	C4P4T4T6	60	right anterior central gyrus around hand area	9.87 (4.39)	Yes	right frontal	Post surgical cavity in right frontal and temporal pole	N/A	(1) behavior arrest, left arm atonic, left hemibody involuntary movement, vocalization, bimanual automatism, rapid postictal recuperation (20 s) (2) staring (few second)	right front-central	N/A	anterior and posterior central gyrus around hand area

Table 1 (*continued*)

Patient ID	Spike field	Number of event	Location with maximum BOLD activation	Max *t*-value (FDR)	Concordant with pSOZ	pSOZ	MRI finding	SEEG	Seizure description (sz duration)	ictal EEG	PET	MEG
9	F7T3F9T9Fp1F3	17	leftt hippocumpus	6.85 (4.59)	Yes	left temporal	normal	N/A	déjà vu aura, staring, dysphasia, postictal rapid dysphasic recuperation (1 min)	left front-temporal	N/A	N/A
	F7T3F9T9	94	leftt hippocumpus	9.69 (4.42)	Yes							
10	T3T5T9P9	40	leftt superior temporal	5.91 (4.92)	Yes	left temporal	FLAIR high intensity in left temporal pole and mesial temporal area.	N/A	nocturnal, staring, oural and manual automatism, right arm dystonic posture, right leg pedaling movements (1 min)	left posterior temporal	N/A	N/A
	F7T3T5F9T9P9	67	leftt superior temporal	6.76 (4.48)	Yes							
	Fp1F7F9Fp2	7	leftt thalamus	5.52 (4.55)	No							
11	C4	58	leftt fusiform	4.88 (4.55)	No	right frontal	right hemimegalencephaly Post surgical cavity in right orbitfrontal	N/A	(1) bilateral asymmetric tonic posture with left dominancy (10 s) (2) right head version, tonic posture like figure of 4, peddaling, vocalization (60 s)	right frontal	N/A	N/A
	Fp2	6	left frontal pole	5.55 (4.75)	No							
	Fp1F3F7Fp2FzF9T3T5	1	right fusiform	7.96 (4.42)	No							
	Fp2Fp1F4F3F8T4Fz	6	right thalamus	10.1 (4.31)	No							
12	F4C4FzCz	22	left lingual gyrus	5.03 (4.66)	No	right frontal	FCD in right superior frontal	N/A	nocturnal, fear aura, agitation, right manual automatism, vocalization, dystonic left hand (20 sec)	right front-central	N/A	N/A
	Fp1F3F4C4FzCzFp2	33	right white matter in anterior horn of lateral ventricle	6.22 (4.77)	No							
13	T4F8F10T10	50	left orbitfrontal	4.89 (4.54)	No	right temporal (near face)	Post surgical cavity in right frontal	N/A	(1) left facial tonic movement (2) manual automatism, left facial tonic movement, right head version (30 s)	right temporal-centro-parietal	N/A	N/A
	F7T3F9T9	5	left temporal pole	5.77 (4.68)	No							
	T4	44	left posterior superior temporal	6.93 (5.10)	No							
	T4F10T10C4P4	44	right posterior superior temporal	8.92 (4.46)	Yes							
14	F7T3F9T9	12	right hippocampal gyrus	5.33 (4.42)	No	left posterior quadrant	bil-trigonal PVNH	N/A	no aura, behavior arrest, manual automatism, repeating some words (2 min)	left posterior quadrant	N/A	N/A
	T5P9O1P3	8	left posterior middle temporal	6.17 (4.66)	Yes							
	F8T4F10T10	32	left anterior cingulate	6.52 (4.58)	No							
15	F3F7T3F9T9	213	leftt temporal pole	6.76 (4.76)	Yes	leftt temporal	atrophy in the right basal ganglia	N/A	strange sensation in right hemibody	left front-temporal	N/A	N/A
16	F8T4F10T10C4P4T6P10	44	right temporal pole	13.36 (4.20)	No	right frontal	Post surgical cavity in right frontal AVM	N/A	(1) left arm strange sensation, left side clonic movement, unresponsive (20 s) (2) GTC	right front-temporal	N/A	N/A

(*continued on next page*)

Table 1 (*continued*)

Patient ID	Spike field	Number of event	Location with maximum BOLD activation	Max *t*-value (FDR)	Concordant with pSOZ	pSOZ	MRI finding	SEEG	Seizure description (sz duration)	ictal EEG	PET	MEG
17	P9O1T5P3	275	left temporal-occipital junction	7.67 (4.85)	Yes	left front-tempero-occipital	left front-tempero-occipital forcal cortical dysplasia Post surgical cavity in left temporo-parieto-occipital	N/A	no aura, oral automatism, staring, vocalization (30 sec)	left temporo-parietato-occipital	lef hemisphere with maximum over the temporal occipital region	N/A
	P9T5T3P3O1	107	left inf orbit-frontal	8.13 (4.76)	Yes							
	F7T3F9T9	26	left inf orbit-frontal	5.78 (5.00)	Yes							
	F7T3F9T9Fp1F3Fz	22	left inf orbit-frontal	8.26 (4.62)	Yes							
18	F7T3T5F9T9P9	55	left anterior temporal	12.6 (4.28)	Yes	left temporal	small left hipocumpus	N/A	auditory hullcination, dysphasia, (4 s)	not recorded	N/A	N/A
19	F8T4F10T10	56	right frontal pole	7.6 (4.46)	No	right temporal	right temporal, bil-occipital nodular heterotopia	nodule in right fusiform	behavior arrest, left head version, both arm tonic posture (30 s)	right front-temporal	N/A	N/A
20	Fp1Fp2	17	left temporal-occipital junction	5.01 (4.81)	No	left temporal	focal cortical dysplasia near anterior horn in lt lateral ventricle	N/A	staring, oral automatism, agitation (3 min)	left temporal	**N/A**	**N/A**
	Fp1F3Fp2F4	66	white matter near right lateral ventricle	14.38 (4.17)	No							
21	C3T3P3T5P9	11	left temporal (PVNH)	6.48 (4.84)	Yes	left temporal (PVNH)	subependimal NH at left posterior horn of lateral ventricle	N/A	staring, GTC (2 min)	no data	N/A	N/A
22	T6P10P4O2	45	left anterior temporal	6.54 (4.44)	No	right temporal	subependimal NH at inferior horn of right lateral ventricle	N/A	no aura, agitation, manual automatisms	right posterior temporal	right temporal	N/A
	T6P10P4O2T4T10	18	right fusiform	10.52 (4.32)	Yes							
	T6P10P4O2T4T10F8F10	58	right fusiform	13.49 (4.21)	Yes							
23	F8T4F10T10	39	right inferior orbitfrontal	6.07 (4.61)	Yes	right frontal	normal	right post central gyrus and right inferior orbitfrontal	left arm tonic movement, unresponsive (50 s)	right front-temporal	N/A	N/A
	F8T4F10T10T6P10	10	right inferior orbitfrontal	6.50 (4.48)	Yes							
	Fp2F4F8T4F10T10T6P10C4	41	right inferior orbitfrontal	10.41 (4.57)	Yes							
24	T4T6F10T10	107	right middle temporal	9.53 (4.44)	Yes	right temporal	right temporal neurocycticerosis	N/A	Spinning sensation followed by visual phenomenon, dysphasia, left head version, GTC, postictal left arm weakness (3 min)	right front-temporal	right posterior temporal	N/A
25	C3P3CzPz	324	left superior frontal (premotor)	9.47 (4.51)	Yes	left prefrontal	FCD in left prefrontal	N/A	(1) strage sensation in right hand (2) right arm tonic movement, dysphasia, unresponsive (20 s) (3) GTC	unclear, obscured by artifact	N/A	N/A

Table 1 (*continued*)

Patient ID	Spike field	Number of event	Location with maximum BOLD activation	Max *t*-value (FDR)	Concordant with pSOZ	pSOZ	MRI finding	SEEG	Seizure description (sz duration)	ictal EEG	PET	MEG
26	Fp1F3Fp2F4F8FzF7T3F8F9T9F10Cz	7	right anterior cingulate	6.67 (4.66)	Yes	right mesial frontal	FCD in right mesial frontal	right anterior and posterior cingulate/ presuneus	vocalization, staring, facial grimacing, left arm tonic posture (30 s)	bilateral frontal with right dominancy	anterior and posterior cingurate gyrus	N/A
	Fp1F3F4FzF7F8C3Cz	236	right anterior cingulate	32.90 (4.10)	Yes							
27	F8F10T10T4	19	right temporal pole	5.58 (5.08)	Yes	right temporal	encephalocele in right temporal pole	N/A	staring, manual automatism, discommunication. (30 s)	right temporal	N/A	N/A
28	F8T4T6	13	left inferior parietal lobe	5.07 (4.93)	No	right frontal	FCD in right superior frontal and operculum	N/A	facial strange sensation, left head version, left side tonic movoment, postictal dysaphasia. (20 s)	right front-temporal	normal	N/A
	Fp2F8F10	24	right operculum	11.31 (4.39)	Yes							
	Fp2F4F8T4F10T10T6P10	11	right superior temporal	16.75 (4.33)	Yes							
29	F7F9T3T9	10	left lingual gyrus	5.36 (4.44)	No	right temporal	encephalocele in bilateral temporal base	N/A	indescribable sensation, staring, bilateral manual automatism (80 s)	right front-temporal	normal	N/A
	T5P9	18	right anterior cingulate	5.93 (4.80)	No							
	T4T6P10T10	4	right hippocampus	5.74 (4.81)	No							
	T6P10	4	left putamen	4.86 (4.42)	No							
30	F7T3F9T9T5P9	30	left fusiform	6.36 (4.95)	Yes	left temporal	normal	N/A	(1) unresponsive (15 s) (2) loud vocalization, tonic-clonic movement from mouth to limbs (60 s)	left temporal	N/A	N/A

GTC = generalized tonic-clonic seuzres, FCD = forcal cortical dysplasia, PVNH = periventricular npdule heterotopia, NH = nodule heterotopia.

2.4. Statistical analysis

The Wilcoxon rank sum test was used for comparison of categorical data. $p < 0.05$ was considered statistically significant. All statistical analyses were performed using JMP 11 (SAS Institute Inc., U.S.A) and Matlab (Math Works, Inc.).

A binomial test was used to assess whether the concordance between the BOLD response and the SOZ was associated to the depth of the SOZ. In a binomial test the null hypothesis assumes the concordance is the same for superficial and depth SOZ, and the binomial distribution is used to compute the probability of the difference in concordance between the groups being as observed or greater.

3. Results

Among 109 consecutive studies from April 2015 to March 2018, 40 studies were excluded for the following reasons: no spike during EEG-fMRI scan in 15 studies, no significant BOLD change in 8, no positive activation in 3, idiopathic generalized epilepsy in 7, multifocal epilepsy in 3, making it difficult to mark IEDs due to artifact or the occurrence of multiple seizures in 3, difficult to identify the significant BOLD change in anatomical image due to poor co-registration caused by excessive motion artifact in one. From 69 studies in 64 patients, we excluded the 5 duplicated studies by removing the study with the smaller number of IEDs. Finally, 64 studies in 64 patients with refractory localization-related epilepsy were evaluated. In these 64 studies, there were 157 types of IEDs, characterized by their spatial distribution.

3.1. Significant value in BOLD changes

In 157 types of IEDs, *t*-values of the primary cluster were above FDR in 109 types, *t*-values were above the 3.1 threshold but below FDR in 43 types. The remaining 5 types had no significant positive activation. Comparing median values, the number of IEDs was statistically significantly higher in the types with *t*-value above FDR than in the types with *t*-value below FDR ($p < 0.001$) (Fig. 2). On the other hand, there was no statistically significant difference between these groups in terms of IED spatial extent, as assessed by the number of electrodes involved ($p = 0.307$).

3.2. BOLD changes concordant with pSOZ

Among the 109 IED types from 58 patients with a primary cluster above the FDR, 63 types occurred in the 30 patients in whom a pSOZ could be defined. In these 63 types, the primary cluster in 36 types was concordant with the pSOZ and it was discordant in the remaining 27 types (Table 1).

Examples of the activation clusters in a patient with one type of IED concordant and another discordant with the pSOZ are displayed on Fig. 2. The primary cluster generated by IEDs in T6-P10-P4-O2 is located in the left anterior temporal lobe, which is discordant with the pSOZ. On the other hand, the primary cluster generated by IEDs in a more extended distribution (T6-P10-P4-O2-T4-T10) is located in the right fusiform gyrus, cortex close to the periventricular nodular heterotopia and considered to be concordant with the pSOZ.

The types of IEDs concordant with the pSOZ had a statistically significantly larger extent on scalp EEG than the types discordant with the pSOZ ($p < 0.001$) (Fig. 3). We also tested this relation between the spatial extent of IEDs and concordance with the pSOZ in the situation where the 10-10 electrodes (F9, T9, P9, F10, T10 and P10) were not considered (they were removed from the analysis if they had been recorded), to eliminate a confounder since the electrode coverage with the 10-10 electrodes is denser in the temporal region. When excluding these 10-10 electrodes, the result was similar: the types of IEDs concordant with the pSOZ had a significantly larger extent on scalp EEG than the types discordant with the pSOZ ($p = 0.006$). The number of IEDs was also significantly different between these groups ($p = 0.0029$).

For the assessment whether the spatial extent of IEDs and the concordance were affected by the depth of the pSOZ, we classified the patients with a pSOZ in mesial temporal and cingulate region as deep (Pt No1, 7, 9, 22, 26 and 30) or the region close to skull as superficial (others). From the 63 types with activations above FDR, the proportion of concordance with the pSOZ was not statistically different in deep and superficial structures (73% (8/11) concordance for deep structures, 54 % (28/52) concordance for superficial structures ($p = 0.23$, binomial test).

4. Discussion

IEDs related BOLD responses in EEG-fMRI are considered as localizing the irritative zone, which is defined as the area of cortical tissue generating IEDs (Kobayashi et al., 2005, Luders et al., 2006, Salek-Haddadi et al., 2006, Jacobs et al., 2008, Tyvaert et al., 2008). These BOLD responses have also been demonstrated to be in many cases a good predictor of the SOZ defined by intracerebral EEG (Thornton et al., 2011, Khoo et al., 2017). However, EEG-fMRI does not reveal the SOZ or epileptogenic zone in all patients with refractory epilepsy. A report showed that widely distributed discordant regions of IED-related hemodynamic change appear to be associated with a widespread SOZ and poor postsurgical outcome (Thornton et al., 2011). Another report indicated, in multifocal and unknown seizure onset defined by SEEG, the maximum BOLD is not always the SOZ because HFOs were not restricted to the region of maximum BOLD response (Gonzalez Otarula et al., 2018). In this study, we tried to identify factors that are predictive of an accurate localization of the pSOZ when performing an EEG-fMRI study. If such factors can be identified, they will help in assessing how much confidence we can place in a result.

For this study, we analyzed separately all IED types according to their spatial extent because we wanted to see if some types are more likely than others to lead to accurate results. Given how we defined “IED type”, most patients had several such types but it is important to note that this is not the usual way we analyze EEG-fMRI studies. If a patient has independent IEDs in the two hemispheres, we obviously analyze them as separate event types. However, if a patient has events with the same maximum but slightly different extents, we usually analyze these events together as one type. When EEG-fMRI was used in other studies, the concordance between the maximum BOLD and the SOZ has been around 70% in patients with difficult-to-localize focal epilepsy (Khoo et al., 2017). This percentage is much higher than in the current study, most likely because we purposefully separated IEDs in different types even if they were generally concordant events. Once grouped, such concordant events yield more significant and therefore more reliable BOLD responses than when separated in smaller groups, as done for the specific purpose of the current study.

First, we found that the number of IEDs during EEG-fMRI scan is an important factor to obtain reliable results. Second, we demonstrated that IEDs of larger extent reveal the location of pSOZ more precisely than more spatially restricted events. In our EEG-fMRI studies, scalp EEG using 10-20 and 10-10 (F9, T9, P9, F10, T10 and P10) electrode systems are normally used. In this system, the density of the electrodes in the temporal area is higher than in

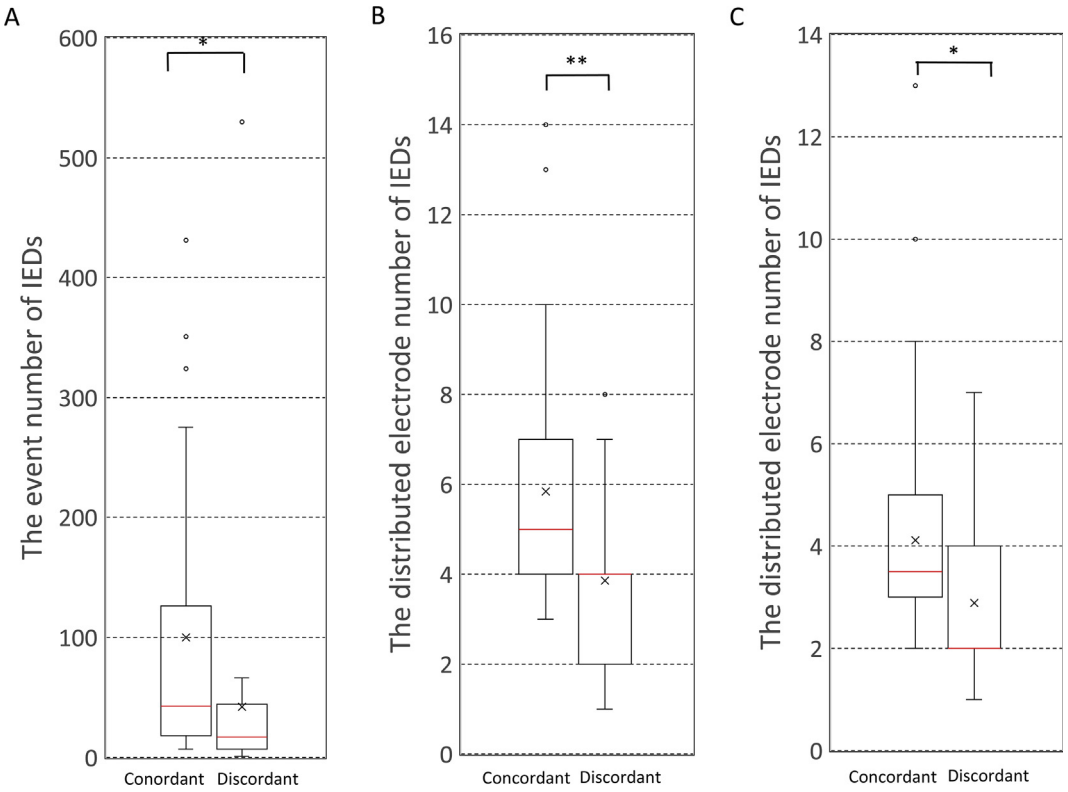

Fig. 3. Number of events and spatial extent of 63 types of IEDs in 30 studies/30 patients during EEG-fMRI, with primary clusters concordant or discordant with the presumed SOZ (pSOZ). The red line corresponds to the median and black boxes extend to the interquartile value. The × marks indicate the mean and the black circles indicate outliers. (A) Number of IEDs when the primary cluster is concordant and discordant with the pSOZ. The IED types concordant with pSOZ had significantly higher numbers of IEDs than the discordant ones (*: $p < 0.05$). (B) Spatial extent of IEDs concordant and discordant with the pSOZ. The IED types concordant with the pSOZ had a significantly larger extent on scalp EEG than the discordant types (**: $p < 0.0001$). (C) Same as (B) but excluding the 10-10 electrodes. The IED types concordant with the pSOZ had a significantly larger extent than the discordant types (*: $p < 0.05$). (For interpretation of the references to colour in this figure legend, the reader is referred to the web version of this article.)

other areas. The result regarding the IED extent was found independently of the inclusion of the 10-10 electrodes.

We have recently demonstrated from the study of BOLD responses and intracerebral EEGs that the maximum BOLD response often corresponds to the spike onset zone, a region where a spike is initiated and from which it propagates (Khoo et al., 2018). This concept can help explain why the concordance between BOLD maxima and the pSOZ is independent of the depth of the BOLD response: from the 63 types with activations above FDR, the proportion of concordance with the pSOZ was not statistically different in deep and superficial structures. The good performance of EEG/fMRI in the case of deep BOLD activation indicates that the methodology allows finding the source of neuronally propagated IEDs. The IEDs could be generated anywhere in the brain, and if they propagate, neuronally, to the lateral neocortex they can be seen in the scalp and used by EEG-fMRI to find the spike onset zone.

From this concept of spike onset zone, one can also imagine that a spike that propagates further, resulting in a more widespread scalp discharge, requires more energy at its source than a spike with a more restricted field. This would imply that the more widespread events have a larger and therefore more likely reliable BOLD response. Note that it is not possible to compare systematically BOLD responses for more or less widespread discharges at the patient level because they usually have a different number of events, which is a major factor in determining the BOLD response. For future studies, we could nevertheless infer that, statistically, a more widespread event is more likely to point to the presumed SOZ than a more restricted event. Although this is counterintuitive, it is in agreement with a recent report showing that EEG synchronization measures are valuable predictors of BOLD fluctuations associated with IEDs (Abreu et al., 2018).

5. Conclusions

The number of IEDs is an important factor in obtaining reliable significant activations in EEG-fMRI. In addition, IEDs with a larger spatial extent are more likely than focal IEDs to reveal an accurate location for the seizure onset zone. This result suggest that widespread discharges require more energy than focal discharges to spread from their source (the spike onset zone), leading to a more marked and reliable BOLD change.

Acknowledgments

This work was supported by grand FDN 143208 of the Canadian Institutes of Health Research. First author received scholarship from Seirei Hamamatsu General Hospital. Dr. H.M.K. was supported by Mark Rayport and Shirley Ferguson Rayport fellowship in epilepsy surgery and was supported by the Preston Robb fellowship of the Montreal Neurological Institute (Canada), research fellowship of the Uehara Memorial Foundation (Japan), travel grants from Osaka Medical Research Foundation for Intractable Diseases (Japan) and Japan Epilepsy Research Foundation (Japan).

Conflicts of interest

None of authors has any conflict of interest to disclose.

References

Abreu R, Leal A, Lopes da Silva F, Figueiredo P. EEG synchronization measures predict epilepsy-related BOLD-fMRI fluctuations better than commonly used univariate metrics. Clin Neurophysiol 2018;129:618–35.

An D, Fahoum F, Hall J, Olivier A, Gotman J, Dubeau F. Electroencephalography/functional magnetic resonance imaging responses help predict surgical outcome in focal epilepsy. Epilepsia 2013;54:2184–94.

Bagshaw AP, Aghakhani Y, Benar CG, Kobayashi E, Hawco C, Dubeau F, et al. EEG-fMRI of focal epileptic spikes: analysis with multiple haemodynamic functions and comparison with gadolinium-enhanced MR angiograms. Hum Brain Mapp 2004;22:179–92.

Baud MO, Perneger T, Racz A, Pensel MC, Elger C, Rydenhag B, et al. European trends in epilepsy surgery. Neurology 2018;91:e96–e106.

Benjamini Y, Hochberg Y. Controlling the false discovery rate: a practical and powerful approach to multiple testing. J R Statist Soc B 1995;57:289–300.

Chowdhury RA, Pellegrino G, Aydin U, Lina JM, Dubeau F, Kobayashi E, et al. Reproducibility of EEG-MEG fusion source analysis of interictal spikes: Relevance in presurgical evaluation of epilepsy. Hum Brain Mapp 2018;39:880–901.

Duncan JS, Winston GP, Koepp MJ, Ourselin S. Brain imaging in the assessment for epilepsy surgery. Lancet Neurol 2016;15:420–33.

Gonzalez Otarula KA, Khoo HM, von Ellenrieder N, Hall JA, Dubeau F, Gotman J. Spike-related haemodynamic responses overlap with high frequency oscillations in patients with focal epilepsy. Brain 2018. https://doi.org/10.1093/brain/awx383.

Guerrini R, Duchowny M, Jayakar P, Krsek P, Kahane P, Tassi L, et al. Diagnostic methods and treatment options for focal cortical dysplasia. Epilepsia 2015;56:1669–86.

Jacobs J, Kobayashi E, Boor R, Muhle H, Stephan W, Hawco C, et al. Hemodynamic responses to interictal epileptiform discharges in children with symptomatic epilepsy. Epilepsia 2007;48:2068–78.

Jacobs J, Rohr A, Moeller F, Boor R, Kobayashi E, LeVan Meng P, et al. Evaluation of epileptogenic networks in children with tuberous sclerosis complex using EEG-fMRI. Epilepsia 2008;49:816–25.

Jayakar P, Gotman J, Harvey AS, Palmini A, Tassi L, Schomer D, et al. Diagnostic utility of invasive EEG for epilepsy surgery: Indications, modalities, and techniques. Epilepsia 2016;57:1735–47.

Khoo HM, Hao Y, von Ellenrieder N, Zazubovits N, Hall J, Olivier A, et al. The hemodynamic response to interictal epileptic discharges localizes the seizure-onset zone. Epilepsia 2017;58:811–23.

Khoo HM, von Ellenrieder N, Zazubovits N, He D, Dubeau F, Gotman J. The spike onset zone: The region where epileptic spikes start and from where they propagate. Neurology 2018;91:e666–74.

Kobayashi E, Bagshaw AP, Jansen A, Andermann F, Andermann E, Gotman J, et al. Intrinsic epileptogenicity in polymicrogyric cortex suggested by EEG-fMRI BOLD responses. Neurology 2005;64:1263–6.

Luders HO, Najm I, Nair D, Widdess-Walsh P, Bingman W. The epileptogenic zone: general principles. Epileptic Disord 2006;8(Suppl 2):S1–9.

Pittau F, Dubeau F, Gotman J. Contribution of EEG/fMRI to the definition of the epileptic focus. Neurology 2012;78:1479–87.

Pittau F, Fahoum F, Zelmann R, Dubeau F, Gotman J. Negative BOLD response to interictal epileptic discharges in focal epilepsy. Brain Topogr 2013;26:627–40.

Salek-Haddadi A, Diehl B, Hamandi K, Merschhemke M, Liston A, Friston K, et al. Hemodynamic correlates of epileptiform discharges: an EEG-fMRI study of 63 patients with focal epilepsy. Brain Res 2006;1088:148–66.

Shih JJ, Fountain NB, Herman ST, Bagic A, Lado F, Arnold S, et al. Indications and methodology for video-electroencephalographic studies in the epilepsy monitoring unit. Epilepsia 2018;59:27–36.

Thornton R, Vulliemoz S, Rodionov R, Carmichael DW, Chaudhary UJ, Diehl B, et al. Epileptic networks in focal cortical dysplasia revealed using electroencephalography-functional magnetic resonance imaging. Ann Neurol 2011;70:822–37.

Tyvaert L, Hawco C, Kobayashi E, LeVan P, Dubeau F, Gotman J. Different structures involved during ictal and interictal epileptic activity in malformations of cortical development: an EEG-fMRI study. Brain 2008;131:2042–60.

Worsley KJ, Liao CH, Aston J, Petre V, Duncan GH, Morales F, et al. A general statistical analysis for fMRI data. Neuroimage 2002;15:1–15.